TECHNICAL PAPER

Vibration reduction in vertical washing machine using a rotating dynamic absorber

Rafael Onohara Campos · Rodrigo Nicoletti

Abstract Most of the vibration problems in vertical washing machines occur during the water extraction process (spinning stage), when high unbalance forces act on the system. The unbalance forces result from the combination of high rotating velocities and the uneven, and unpredictable, mass distribution of the clothing in the machine basket. Hence, reducing system response to unbalance is a way of improving not only the vibration performance of the washing machine, but also customer satisfaction. One of the ways of reducing system response is via dynamic absorbers which work in a passive way, thus not requiring a control system, but excitation frequency must be constant and known. In this work, a rotating vibration absorber is tested for reducing lateral vibration during the spinning process of an 8-kg capacity washing machine. The vibration absorber is mounted on the rotating basket of the machine, whirling at the same velocity of the basket. A model for the rotating dynamic absorber is proposed and coupled to the model of the washing machine. Numerical and experimental results are obtained concerning unbalance response in the conditions of the spinning process. A comparison between the systems with and without the rotating dynamic absorber shows significant reduction in the lateral vibration of the machine basket when the absorber is used. Because the efficiency of vibration absorbers does not depend on the amplitude of excitation forces, vibration reduction occurs irrespective of the unbalance condition.

R. O. Campos · R. Nicoletti (✉)
School of Engineering of São Carlos, University of São Paulo,
São Carlos, SP 13566-590, Brazil
e-mail: rnicolet@sc.usp.br

List of symbols

$\mathbf{a}$	Absolute acceleration vector, m/s^2
d	Suspension linear damping coefficient, N s/m
d_a	Damping coefficient of the absorber, N s/m
d_t	Suspension angular damping coefficient, N m s/rad
e_D	Unbalance eccentricity, m
E	Young modulus, N/m^2
$\mathbf{f}$	Force vector, N
$\mathbf{h}_A$	Angular momentum vector in respect to A, kg m^2/s
$\mathbf{i}, \mathbf{j}, \mathbf{k}$	Unitary vectors of reference frame
I	Area moment of inertia, m^4
I_T	Lateral mass moment of inertia, kg m^2
I_P	Polar mass momento of inertia, kg m^2
$\mathbf{I}_A$	Inertia tensor in respect to A, kg m^2
m	Total mass of the system, kg
m_a	Mass of the dynamic absorber, kg
m_D	Unbalance mass, kg
$\mathbf{m}$	Moment vector, N m
k	Suspension linear stiffness coefficient, N/m
k_a	Stiffness coefficient of the absorber, N/m
k_t	Suspension angular stiffness coefficient, N m/rad
L	Distance between points A and CG, m
L_D	Distance between points A and unbalance, m
$\mathbf{r}$	Displacement vector, m
$\mathbf{T}_\beta$	Transformation matrix for reference I to reference B1
$\mathbf{T}_\gamma$	Transformation matrix for reference B1 to reference B2
$\mathbf{v}$	Absolute velocity vector, m/s
$\mathbf{w}$	Weight vector, N

x, y Coordinates of point A, m

x_a, y_a Coordinates of absorber center of gravity, m

Greek symbols

β Rotation about axis X, rad

γ Rotation about axis Y_1

$\dot{\phi}$ Basket whirling velocity, rad/s

ω_a Natural frequency of the absorber, rad/s

$\boldsymbol{\omega}$ Absolute angular velocity vector of the basket, rad/s

$\boldsymbol{\Omega_2}$ Absolute angular velocity of reference $B2$, rad/s

Subscripts

a Relative to rotating dynamic absorber

A Relative to point A

B Relative to point B

$B1$ Relative to first auxiliary reference frame

$B2$ Relative to second auxiliary reference frame

C Relative to point C

CG Relative to center of gravity

D Relative to unbalance

I Relative to inertial reference frame

S Relative to suspension

W Relative to weight

1 Introduction

Rotating machines can be found in a huge variety of products, used in almost every branch of the productive chain (from raw materials prospecting till final product manufacturing). Considering the widespread application of rotating machines, one can infer their importance in the productive chain and the economic consequences of their ill functioning due to excessive rotor lateral vibration.

In this context, investigations on control of rotor lateral vibrations have been done, focusing on both passive and active control. Active control requires the design of sensors and actuators, and the implementation of feedback control systems. In this case, the machine must be originally designed to have such sensing and actuating systems, resulting in a more elaborated and costly project, but with significant results in vibration reduction. Some examples of active control in rotating machines are the application of magnetic bearings [11], hydraulic chamber actuators [2], geometry compliant bearings [23], active hydrostatic bearings [20], and active lubricated bearings [15].

The passive control of vibration in rotating machines is a lower cost alternative compared to the active control. In this case, vibration control is implemented in open loop circuit, not needing any sensor or actuator system. The first step in the passive control of rotor lateral vibrations is finding the optimum damping reserve of the bearings and supports [4, 5, 10]. If the damping reserve of bearings and supports cannot acceptably reduce rotor lateral vibrations, one can adopt complementary devices like squeeze-film dampers [18] or seal dampers [24]. These complementary devices are designed to increase damping reserve of the bearings of the rotating machine in a passive way.

The examples of passive control mentioned above are broad band approaches, because they try to reduce rotor vibration in a wide range of frequencies. Considering that many rotating machines operate at narrow frequency ranges, one can apply modal attenuation techniques. Modal attenuation techniques refer to the design of machines, or devices to be mounted on the machines, aiming at reducing to a minimum the machine forced response under specific excitation frequencies [14, 17]. Hence, this is an alternative approach to the broad band strategies mentioned above. The technique tries to locate anti-resonances of the rotor lateral mode in specific frequency ranges of interest, thus reducing rotor response. Dynamic vibration absorbers are an example of such modal attenuation devices.

One can find in literature different ways of using dynamic vibration absorbers in rotating machines. For example, if the rotor is mounted on flexible bearings, the absorber can be fixed on the bearing housings to reduce rotor lateral vibrations [12]. The absorber can also be mounted on the rotor, to attenuate rotor lateral vibration or blade vibration [16]. The difference between both approaches (absorber mounted on the housing or on the rotor) is that, in the latter, the absorber whirls together with the rotor, which gives advantages such as the possibility to observe and control parametric vibration [19].

Concerning rotating dynamic absorbers mounted on the rotor, centrifugal pendulum absorbers [7, 22] and ball balancers [1, 13] are proposed to control rotor torsion vibration. In order to control rotor lateral vibration, one can rely on hydraulic balancers [3, 21] and on ring absorbers [6]. Due to their simplicity and low cost, hydraulic balancers, more specifically Leblanc balancers, are commonly adopted in vertical axis washing machines to reduce lateral vibration of the rotor during centrifugation (water extraction process). However, due to its working principle, the Leblanc balancers can only partially reduce lateral vibration.

In this work, a rotating ring dynamic absorber of simple geometry is mounted on the basket of a vertical axis washing machine. The idea is that the absorber work at the rotating frequency of the basket during the water extraction process (spinning stage or centrifugation). The unbalance forces in spinning stage result from the combination of high rotating velocities and the uneven, and unpredictable, mass distribution of the clothing in the machine basket. Hence, considering that the efficiency of vibration absorbers does not depend on the amplitude of excitation forces, vibration reduction can occur
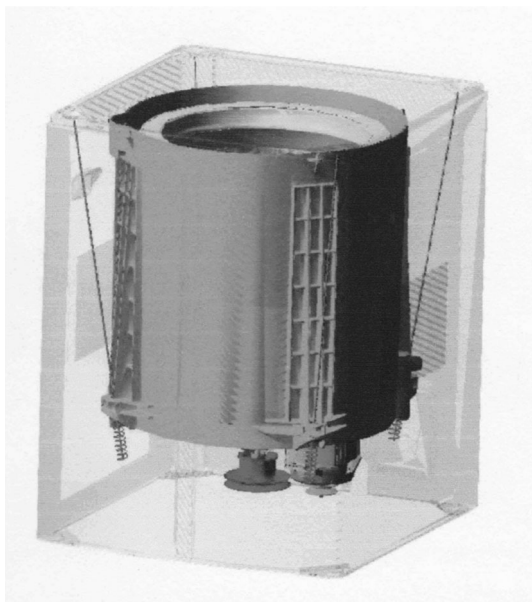
Fig. 1 Vertical washing machine in study [9]

irrespective of the unbalance condition, in theory. By tuning the absorber in the rotating frequency of the spinning stage, one expects that vibration energy of the basket be transferred to the absorber. Less vibration energy in the basket means less dynamic loading in the mounts, resulting in less overall noise and vibration of the washing machine structure.

2 The vertical washing machine with dynamic absorber

The washing machine in study is shown in Fig. 1. It is a vertical axis washing machine of 8 kg capacity, composed of a tank supported by four suspension rods. Beneath the tank is mounted the electric motor that impels the whirling basket inside the tank. The system (tank + motor + basket) is free to translate and rotate around the attachment points of the suspension (lower part of the tank), i.e. there are no restrictions in the upper part of the tank/basket.

The proposed rotating ring dynamic absorber is mounted on the basket of the machine, in order to whirl at the same velocity of the basket (Fig. 2). It is composed of inertial mass and elastic elements connecting the mass to the top of the basket. The inertial mass (steel ring) weighs approximately 5 kg and the elastic elements are eight steel rods, of 2.5 mm diameter. The rods are bolted to the top of the basket, whereas the inertial mass is bolted to the rods (Fig. 2). Hence, the elastic elements limit the degrees-of-freedom of the absorber to translational degrees-of-freedom with respect to the basket.
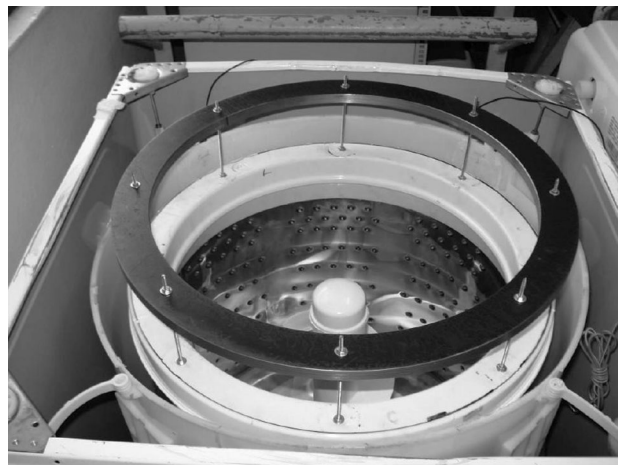

Fig. 2 Rotating dynamic absorber mounted on the top of the basket of the washing machine

3 Experimental setup

The vibration performance of the washing machine is analyzed by acceleration measurements during the spinning stage. These acceleration measurements are done at four distinct points of the machine: two points in orthogonal directions in the bottom plane of the machine, and two points in orthogonal directions in the upper plane of the machine (Fig. 3). Piezo accelerometers are mounted at the measurement points, in the tank of the machine. Previous experimental results, presented by Ioriatti [9], at the same points in a similar machine showed that the tank is rigid enough to perform the analysis: no distinguishable components were found at higher frequencies in the waterfall diagram of the system (except a strong $1 \times \Omega$ component in the measurement signals). This is evidence that higher
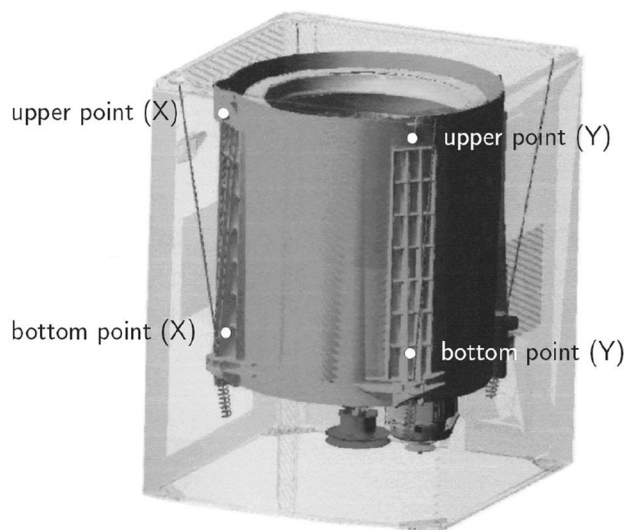

Fig. 3 Measurement points in the washing machine

Fig. 4 Unbalance load mounted in the inner surface of the basket

Fig. 5 Reference frames and rotations adopted in the mathematical modeling of the vertical washing machine

natural frequencies of the structure are not significantly excited by the unbalance.

The signals are acquired by an NI USB 6009 acquisition board, at a sample rate of 1 kHz and acquisition period of 3 s, and filtered at 300 Hz cut-off frequency. Two different loading conditions are tested: 250 g unbalance, and 500 g unbalance. The unbalance loads are imposed by masses of 250 and 500 g, mounted in the inner surface of the basket, as shown in Fig. 4. The measurements are done after reaching the steady-state operation of the machine during the spinning stage (centrifugation process). The orbits of the basket in the measurement planes are obtained by numerically integrating the acceleration data in time.

4 Mathematical modeling of the vertical washing machine

The system tank + motor + basket is modeled by rigid body dynamics. In order to represent the translations and rotations of the system, one adopts the reference frames shown in Fig. 5. The inertial reference frame I (XYZ) has origin in **O**, which is the center of the machine in the plane of the suspension attachments in the lower part of the tank. A first auxiliary reference frame B1 ($X_1Y_1Z_1$) has origin in point **A** (center of the tank in the plane of the suspension attachments) and presents a translation in plane XY and a rotation β around axis X of the inertial frame. A second auxiliary reference frame B2 ($X_2Y_2Z_2$), with origin in point **A**, is attached to the tank, following its movements, and presents a rotation γ around axis Y_1 of reference frame B1. The whirling velocity of the basket is represented by an angular velocity $\dot{\phi}$ in Z_2 axis, and the center of gravity lies in the same axis Z_2.

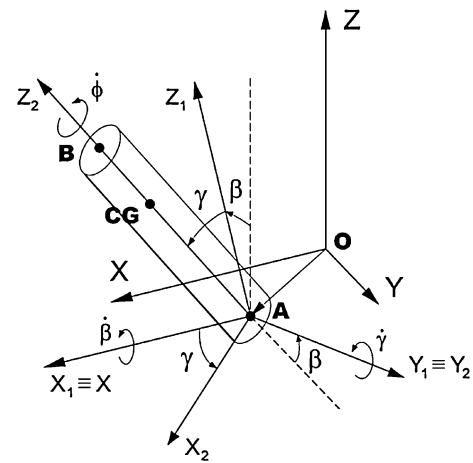The system is subjected to its weight, the restoring forces and moments of the suspension, and the dynamic forces of the unbalance (clothing in the basket). Hence, one can write the conservation laws as follows:

$$m\,_I\mathbf{a}_{\mathrm{CG}} = \,_I\mathbf{w} + \,_I\mathbf{f}_S + \,_I\mathbf{f_D} \tag{1}$$

$$\frac{\mathrm{d}}{\mathrm{d}t}\left(_{B2}\mathbf{h}_A\right) + \,_{B2}\Omega_2 \times_{B2}\mathbf{h}_A = \,_{B2}\mathbf{r}_{\mathrm{CG/A}} \times \,_{B2}\mathbf{w} + \,_{B2}\mathbf{m}_S \\ + \,_{B2}\mathbf{r}_D \times \,_{B2}\mathbf{f}_D \tag{2}$$

where $_{B2}\mathbf{h}_A = \,_{B2}\mathbf{I}_{A\ B2}\,\boldsymbol{\omega} + \mathbf{m}\,_{B2}\mathbf{r}_{\mathrm{CG/A}} \times \,_{B2}\mathbf{v}_A$.

Considering that the displacement vectors can be defined as:

$$_I\mathbf{r}_A = x\mathbf{i} + y\mathbf{j} \tag{3}$$

$$_I\mathbf{r}_{\mathrm{CG/A}} = \mathbf{T}_\beta^T \mathbf{T}_\gamma^T \,_{B2}\mathbf{r}_{\mathrm{CG/A}} \tag{4}$$

where $_{B2}\mathbf{r}_{\mathrm{CG/A}} = L\mathbf{k}_2$, the absolute acceleration vector of the system center of gravity, described in the inertial frame, is given by:

$$_I\mathbf{a}_{\mathrm{CG}} = \frac{\mathrm{d}^2}{\mathrm{d}t^2}\left(_I\mathbf{r}_{\mathrm{CG}}\right) = \frac{\mathrm{d}^2}{\mathrm{d}t^2}\left(_I\mathbf{r}_A + \,_I\mathbf{r}_{\mathrm{CG/A}}\right) \tag{5}$$

The forces acting on the system are:

$$_I\mathbf{w} = -mg\,\mathbf{k} \tag{6}$$

$$_I\mathbf{f}_S = -k\,_I\mathbf{r}_A - d\,_I\mathbf{v}_A \tag{7}$$

$$_I\mathbf{f}_D = \mathbf{T}_\beta^T\mathbf{T}_\gamma^T\,_{B2}\mathbf{f}_D \tag{8}$$

where

$$_{B2}\mathbf{f}_D = F_{Dx}\mathbf{i}_2 + F_{Dy}\mathbf{j}_2 = m_De_D\dot{\phi}^2\left(\cos\dot{\phi}t\mathbf{i}_2 + \sin\dot{\phi}t\mathbf{j}_2\right).$$

Hence, Eq. (1) results in the following equations of motion:

$$\begin{cases} m\ddot{x} + mL\ddot{\gamma}\cos\gamma = mL\dot{\gamma}^2\sin\gamma - kx + F_{Dx}\cos\gamma \\ m\ddot{y} - mL\ddot{\beta}\cos\beta\cos\gamma + mL\ddot{\gamma}\sin\beta\sin\gamma = \\ -mL\dot{\beta}^2\sin\beta\cos\gamma - 2mL\dot{\beta}\dot{\gamma}\cos\beta\sin\gamma \\ -mL\dot{\gamma}^2\sin\beta\cos\gamma - ky + F_{Dy}\cos\beta + F_{Dx}\sin\beta\sin\gamma \end{cases} \tag{9}$$

The inertia tensor $_{B2}\mathbf{I}_A$ is represented in reference frame $B2$, which is aligned to the principal axes of inertia of the system. Hence, the inertia tensor is diagonal and time independent.

The absolute angular velocity vectors of the auxiliary reference frame $B2$ and of the system are, respectively:

$$_{B2}\mathbf{\Omega}_2 = \mathbf{T}_{\gamma\,B1}\dot{\boldsymbol{\beta}} + {}_{B2}\dot{\boldsymbol{\gamma}} \tag{10}$$

$$_{B2}\boldsymbol{\omega}_2 = \mathbf{T}_{\gamma\,B1}\dot{\boldsymbol{\beta}} + {}_{B2}\dot{\boldsymbol{\gamma}} + {}_{B2}\dot{\boldsymbol{\phi}} \tag{11}$$

where $_{B1}\dot{\boldsymbol{\beta}} = \dot{\beta}\mathbf{i}_1$, $_{B2}\dot{\boldsymbol{\gamma}} = \dot{\gamma}\mathbf{j}_2$, and $_{B2}\dot{\boldsymbol{\phi}} = \dot{\phi}\mathbf{k}_2$.

The restoring moment of the suspension is given by:

$$_{B2}\mathbf{m}_S = \mathbf{T}_{\gamma}\,\mathbf{T}_{\beta\,I}\mathbf{m}_S \tag{12}$$

where $_I\mathbf{m}_S = -\left(k_t\beta + d_t\dot{\beta}\right)\mathbf{i} - (k_t\gamma\cos\beta + d_t\dot{\gamma}\cos\beta)\mathbf{j}$.

Hence, Eq. (2) results in the following equations of motion:

$$\begin{cases}
I_T\ddot{\beta}\cos\gamma - mL\ddot{y}\cos\beta = (2I_T - I_P)\dot{\beta}\dot{\gamma}\sin\gamma \\
\qquad - mL\dot{y}\dot{\beta}\sin\beta\cos^2\gamma - I_P\dot{\phi}\dot{\gamma} + mL\dot{x}\dot{\beta}\sin\gamma\cos\gamma \\
\qquad + mgL\sin\beta - k_t\beta\cos\gamma - k_t\gamma\sin\beta\cos\beta\sin\gamma \\
\qquad - d_t\dot{\beta}\cos\gamma - d_t\dot{\gamma}\sin\beta\cos\beta\sin\gamma - L_D F_{Dy} \\
I_T\ddot{\gamma} + mL\ddot{x}\cos\gamma + mL\ddot{y}\sin\beta\sin\gamma = mL\dot{x}\dot{\gamma}\sin\gamma \\
\qquad - mL\dot{y}\dot{\gamma}\sin\beta\cos\gamma + (I_P - I_T)\dot{\beta}^2\sin\gamma\cos\gamma \\
\qquad + I_P\dot{\phi}\dot{\beta}\cos\gamma + mgL\cos\beta\sin\gamma + k_t\gamma\cos^2\beta \\
\qquad - d_t\dot{\gamma}\cos^2\beta + L_D F_{Dx}
\end{cases} \tag{13}$$

Equations (9) and (13) are the non-linear equations of motion of the vertical axis washing machine. These equations can be rearranged in matrix form:

$$\mathbf{A}(\beta,\gamma)\ddot{\mathbf{s}} = \mathbf{g}\left(\mathbf{s}, \dot{\mathbf{s}}, \dot{\phi}, F_{Dx}, F_{Dy}\right), \tag{14}$$

where $\mathbf{s} = \{x\,y\,\beta\,\gamma\}^T$ and upper dots refer to time derivatives. From Eq. (14), one can numerically integrate the non-linear equations of motion, by knowing the initial conditions $\mathbf{s}_0$ and $\dot{\mathbf{s}}_0$.

5 Mathematical modeling of the rotating dynamic absorber

The same reference frames can be used to derive the equations of motion of the rotating dynamic absorber. The absorber center of gravity **CGa** can present relative displacements to the basket in the plane X_2Y_2 (translation) around point **C**, as shown in Fig. 6. The movement plane of the absorber (around point **C**) is not the same as that of the top of the basket (point **B**) because of the length of the elastic elements. Because the absorber is attached to the
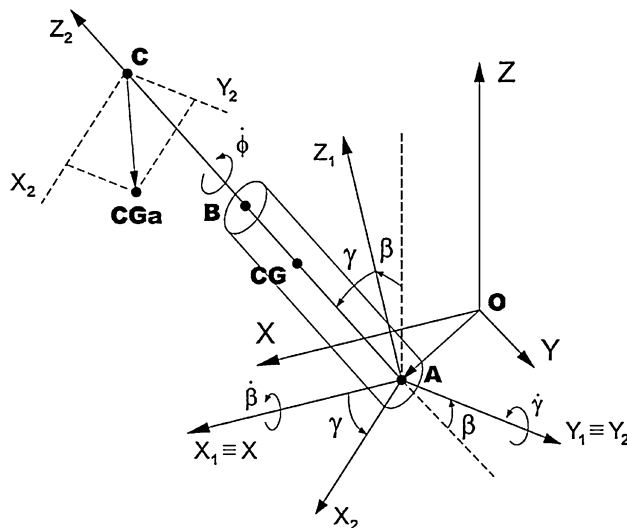

Fig. 6 Reference frames and rotations adopted in the mathematical modeling of the rotating dynamic absorber

basket, rotations are the same as those presented by the basket.

The absorber is subjected to its weight and the restoring forces of the elastic elements. Thus, one can write the conservation law as follows:

$$m_a\,_{B2}\mathbf{a}_{\mathrm{CGa}} = {}_{B2}\mathbf{w}_a + {}_{B2}\mathbf{f}_a \tag{15}$$

By assuming that the moments of inertia of the dynamic absorber are much smaller than those of the machine (tank + motor + basket), the conservation law of the absorber angular momentum is not considered in this analysis.

The displacement vector of the absorber center of gravity can be defined as:

$$_{B2}\mathbf{r}_{\mathrm{CGa}} = \mathbf{T}_{\gamma}\mathbf{T}_{\beta\,I}\,\mathbf{r}_A + {}_{B2}\,\mathbf{r}_{C/A} + {}_{B2}\,\mathbf{r}_{\mathrm{CGa}/C} \tag{16}$$

where $_{B2}\mathbf{r}_{C/A} = L_C\mathbf{k}_2$ and $_{B2}\mathbf{r}_{\mathrm{CGa}/C} = x_a\mathbf{i}_2 + y_a\mathbf{j}_2$.

The absolute velocity and absolute acceleration vectors of the absorber center of gravity, described in the auxiliary frame $B2$, are given by:

$$_{B2}\mathbf{v}_{\mathrm{CGa}} = \frac{\mathrm{d}}{\mathrm{d}t}\left(_{B2}\mathbf{r}_{\mathrm{CGa}}\right) + {}_{B2}\mathbf{\Omega}_2 \times {}_{B2}\mathbf{r}_{\mathrm{CGa}} \tag{17}$$

$$_{B2}\mathbf{a}_{\mathrm{CGa}} = \frac{\mathrm{d}}{\mathrm{d}t}\left(_{B2}\mathbf{v}_{\mathrm{CGa}}\right) + {}_{B2}\mathbf{\Omega}_2 \times {}_{B2}\mathbf{v}_{\mathrm{CGa}} \tag{18}$$

The forces acting on the system are:

$$_{B2}\mathbf{w}_a = \mathbf{T}_{\gamma}\mathbf{T}_{\beta\,B2}\mathbf{w}_a \tag{19}$$

$$_{B2}\mathbf{f}_a = -k_a\,_{B2}\mathbf{r}_{\mathrm{CGa}/C} - d_a\,_{B2}\mathbf{v}_{\mathrm{CGa}/C} \tag{20}$$

where $_I\mathbf{w}_a = -m_a g\mathbf{k}$.

Hence, Eq. (15) results in the following equations of motion:

$$\begin{cases}
m_a\ddot{x}\cos\gamma + m_a\ddot{y}\sin\beta\sin\gamma + m_a\ddot{x}_a + m_aL_B\ddot{\gamma} \\
\quad - m_ay_a\ddot{\beta}\sin\gamma = m_ay\dot{\gamma}\left(\dot{\gamma} - \dot{\beta}\right)\sin\beta\sin\gamma \\
\quad + m_ax_a\left(\dot{\gamma}^2 + \dot{\beta}^2\sin^2\gamma\right) - m_aL_C\dot{\beta}^2\sin\gamma\cos\gamma - k_ax_a \\
\quad + 2m_a\dot{y}_a\dot{\beta}\sin\gamma - d_a\dot{x}_a + m_ag\cos\beta\sin\gamma \\
m_a\ddot{y}\cos\beta + m_ax_a\ddot{\beta}\sin\gamma - m_aL_B\ddot{\beta}\cos\gamma + m_a\ddot{y}_a = \\
\quad - 2m_ax_a\dot{\beta}\dot{\gamma}\cos\gamma + m_ay\dot{\beta}\left(\dot{\beta} - \dot{\gamma}\right)\sin\beta\sin\gamma\cos\gamma \\
\quad - 2m_a\dot{\beta}(\dot{x}_a + L_C\dot{\gamma})\sin\gamma + m_ay_a\dot{\beta}^2 - k_ay_a \\
\quad - d_a\dot{y}_a - m_ag\sin\beta
\end{cases}$$
$$(21)$$

Equation (21) is the non-linear equation of motion of the rotating dynamic absorber mounted on the top of the washing machine basket.

6 Global mathematical model

The global model of the system (washing machine + absorber) can be achieved by rewriting the conservative laws of the machine. Hence, one has:

$$m_I\mathbf{a}_{CG} = {}_I\mathbf{w} + {}_I\mathbf{f}_S + {}_I\mathbf{f}_D - {}_I\mathbf{f}_a \qquad (22)$$

where ${}_I\mathbf{f}_a = \mathbf{T}_\beta^T\mathbf{T}_\gamma^T{}_{B2}\mathbf{f}_a$, and:

$$\frac{\mathrm{d}}{\mathrm{d}t}({}_{B2}\mathbf{h}_A) + {}_{B2}\mathbf{\Omega}_2 \times {}_{B2}\mathbf{h}_A = {}_{B2}\mathbf{r}_{CG/A} \times {}_{B2}\mathbf{w} + {}_{B2}\mathbf{m}_S \\
+ {}_{B2}\mathbf{r}_D \times {}_{B2}\mathbf{f}_D + {}_{B2}\mathbf{r}_{B/A} \\
\times (-{}_{B2}\mathbf{f}_a)$$
$$(23)$$

The difference between Eqs. (1) and (2) and Eqs. (22) and (23) lies on the terms related to the restoring forces of the elastic elements between the absorber and the basket.

Hence, by adding the terms related to the restoring forces of the absorber elastic elements to the equations of motions (9) and (13), and considering the equations of motion of the rotating dynamic absorber (Eq. 21), one arrives to a system of non-linear equations of motion. This system of non-linear equations of motion can be rearranged in matrix form, as follows:

$$\mathbf{B}(\beta, \gamma, x_a, y_a)\ddot{\mathbf{u}} = \mathbf{p}\left(\mathbf{u}, \dot{\mathbf{u}}, \dot{\phi}, F_{Dx}, F_{Dy}\right) \qquad (24)$$

where $\mathbf{u} = \{x\ y\ \beta\ \gamma\ x_a\ y_a\}^T$ and upper dots refer to time derivatives. From Eq. (24), one can numerically integrate the non-linear equations of motion, by knowing the initial conditions $\mathbf{u}_0$ and $\dot{\mathbf{u}}_0$.

Table 1 Parameter values of the vertical washing machine

$m = 30$ kg	$k = 2{,}100$ N/m	$m_D = 250/500$ g
$I_P = 0.632$ kg m^2	$k_t = 100$ N m/rad	$L_D = 0.15$ m
$I_T = 3.658$ kg m^2	$d = 60$ N s/m	$e_D = 0.23$ m
$L = -0.007$ m	$d_t = 10$ N m s/rad	$\dot{\phi} = 13$Hz
$L_B = 0.46$ m		

7 Unbalance response of the system with mistuned absorber

The vertical washing machine in study has parameters whose values are listed in Table 1. At the spinning stage (centrifugation process), the basket whirls at a rotating frequency of 13 Hz. In order to investigate the behavior of the whirling basket, one will focus on the displacements of the basket extremities, i.e. the bottom and the upper extremities of the basket (points **A** and **B** of the mathematical modeling and measuring points).

Considering that the rotating dynamic absorber introduces a mass of 5 kg in the system, the machine in the original condition (without the absorber) would be unloaded by 5 kg. This situation would lead to biased results, and it would not be possible to compare the results to those obtained in the machine with the absorber (system plus 5 kg). Hence, in order to be possible to compare results from the system in the original configuration with those from the system with the absorber, the original system was tested with a mistuned absorber in place. In this case, the ring of the absorber was mounted as close as possible to the
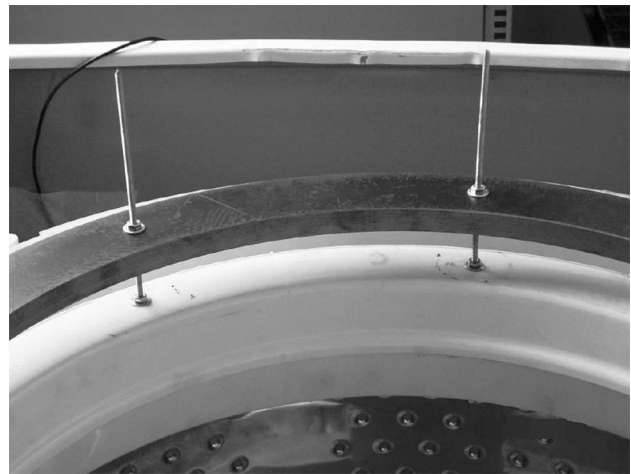

Fig. 7 Mistuned absorber mounted on the washing machine (addition of 5 kg mass in the system)
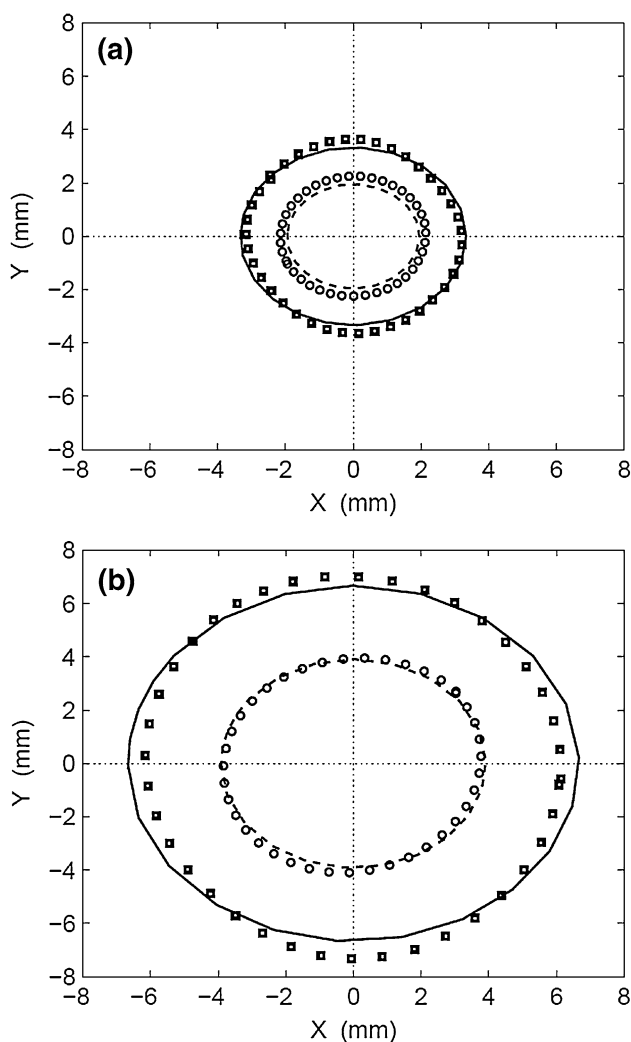
Fig. 8 Comparison between numerical and experimental results of the orbits of the system with mistuned absorber: **a** 250 g unbalance, **b** 500 g unbalance. *continuous line* point A (num.), *circles* point A (exp.), *dashed line* point B (num.), *squares* point B (exp.)
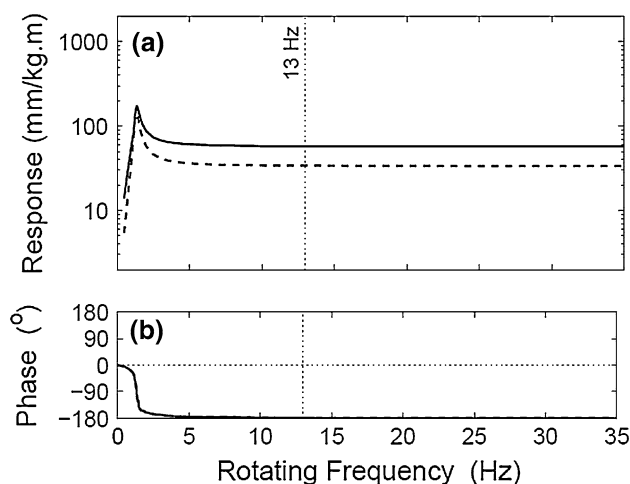

Fig. 9 Unbalance response of the system with mistuned absorber: **a** response per unbalance unit, **b** phase. *continuous line* point A, *dashed line* point B

in both tested conditions of unbalance. In both cases, the orbit of the bottom plane of the basket (dashed line) presents a lower radius than that of the upper plane of the basket (solid line), which is an indication that the basket is presenting a conical whirling mode (inverse cone). Some small deviations between numerical and experimental results are noted in Y direction probably caused by the orthotropy of the suspension stiffness (different torsion stiffness in X and Y directions).

Based on the mathematical model, one can obtain the unbalance response function of the system, shown in Fig. 9. As one can see, the system with mistuned absorber has a critical frequency of 1.4 Hz (Fig. 9a), and it whirls in opposition of phase to the unbalance force at the operational frequency of 13 Hz (Fig. 9b). This behavior is coherent to that of most vertical axis washing machines, where the centrifugation process occurs much above the natural frequency of the system.

8 Unbalance response of the system with working absorber

In the spinning stage, the basket whirls at a rotating frequency of 13 Hz. Hence, the dynamic absorber must have its natural frequency near 13 Hz in order to efficiently work. In this case, theoretically, the equivalent stiffness of the absorber must be:

$$k_a = m_a \omega_a^2 = 33,359.3 \, \text{N/m} \tag{25}$$

which represents a stiffness of 4,169.9 N/m for each rod, considering eight rods in the absorber and an inertial mass of 5 kg. From the theory of Mechanics of Materials [8], a clamped–clamped slender beam (Euler–Bernoulli beam)
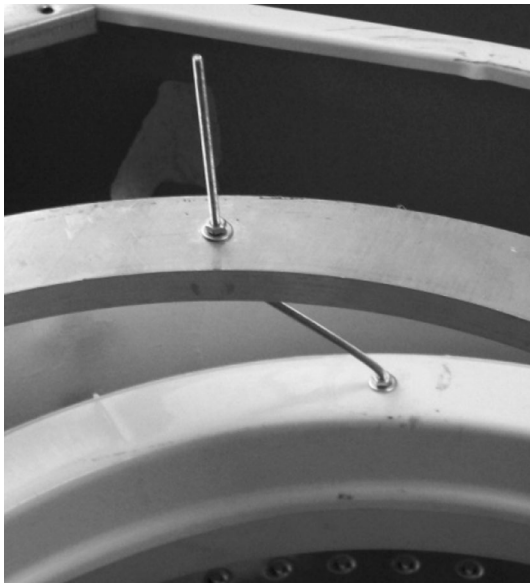
top of the basket (Fig. 7), thus leading to a natural frequency of the absorber much higher than 13 Hz (rotating frequency at the spinning stage). As a result, the mass of 5 kg is introduced in the system, but the absorber does not work because the rods are too stiff.

In this case, one can adopt the equations of motion (14), resultant from Eqs. (9) and (13). The integration of the equations of motion is performed by an explicit fourth order Runge–Kutta algorithm (command ode45 of MAT-LAB software). The system is integrated under operational conditions, subjected to unbalance loads of 250 and 500 g, whose results are presented in Fig. 8a, b in comparison to experimental results.

As one can see in Fig. 8a, b, good agreement to experimental results is achieved with the proposed model,

Fig. 10 Collapsed absorber with 105 mm length rods

subjected to motion in one of its extremities has an equivalent stiffness coefficient of:

$$k_{eq} = \frac{12EI}{\ell^3} \tag{26}$$

Hence, considering a stiffness of 4,169.9 N/m, each rod of the absorber must have a length of $\ell = \sqrt[3]{12EI/k_{eq}} = 105$ mm (distance between the ring and the basket top). In theory, this is the length of the rods that tunes the absorber with the rotating frequency of the machine. In this case, during steady-state operation, one expects a reduction of vibration amplitude of the machine basket and energy be transferred to the absorber.

By testing the washing machine with the absorber with 105 mm rods, energy has been actually transferred to the absorber in such an extent that the dynamic stress in the rods reached the yield limit of strength of the material (Fig. 10). In this case, structural damping was too low to dissipate the vibration energy in the absorber, thus leading the system to present high vibration amplitudes and, as a result, to collapse even before reaching steady-state operation.

For this reason, the system was tested with 95-mm length rods, a slightly mistuned condition of the absorber. In this case, according to Eq. (26), each rod has an equivalent stiffness of 5,635.8 N/m, resulting in a global stiffness of the absorber of 45,086.8 N/m ($\omega_a = 15.1$ Hz). The integration of the equations of motion (24) is, again, performed by an explicit fourth order Runge–Kutta algorithm (command ode45 of MatLab software). The system is integrated under operational conditions, subjected to unbalance loads of 250 and 500 g. The parameters of the

Table 2 Parameter values of the vertical washing machine with absorber

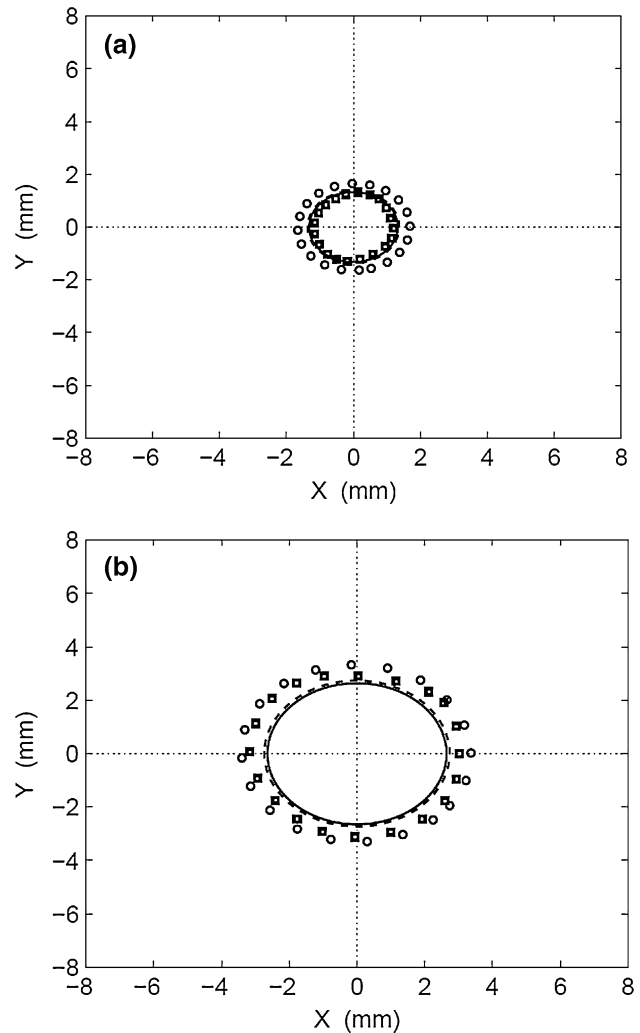|		
$m = 25$ kg	$k = 2{,}100$ N/m	$m_a = 5$ kg
$I_P = 0.632$ kg m^2	$k_t = 100$ N m/rad	$L_C = 0.56$ m
$I_T = 3.658$ kg m^2	$d = 60$ N s/m	$k_a = 45{,}086.8$ N/m
$L = -0.101$ m	$d_t = 10$ N m s/rad	$d_a = 10$ N s/m
$L_B = 0.46$ m		

Fig. 11 Comparison between numerical and experimental results of the orbits of the system with 95-mm rod absorber: **a** 250 g unbalance, **b** 500 g unbalance. *continuous line* point A (num.), *circles* point A (exp.), *dashed line* point B (num.), *squares* point B (exp.)

system with absorber are listed in Table 2, where differences in the values of mass (m) and location of center of gravity (L) are due to the fact that the basket and the absorber are treated as individual bodies in the mathematical modeling. The numerical results are presented in Fig. 11a, b in comparison to the experimental results.
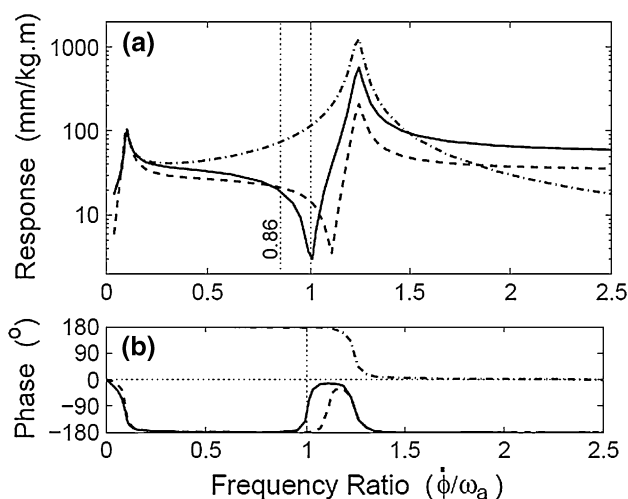
Fig. 12 Unbalance response of the system with absorber: **a** response per unbalance unit, **b** phase. *continuous line* point A, *dashed line* point B, *dash-dotted line* point CGa

As one can see in Fig. 11, a significant reduction of orbit amplitude is achieved with the absorber, especially in the upper plane of the basket, in comparison to results obtained with mistuned absorber (Fig. 8). In the upper plane, up to 69 % reduction in orbit amplitude is achieved for 250 g unbalance, and 57 % reduction for 500 g unbalance. In the bottom plane of the basket, 22 and 13 % reductions of orbit amplitude for 250 and 500 g unbalances, respectively, are observed. In addition, the orbits in the bottom plane have higher amplitudes than those of the upper plane, showing a change of the basket whirling mode. Based on the orbits, in the case of the mistuned absorber, the system presented an inverse cone whirling mode, whereas, in the case of the 95 mm rod absorber, the system presented an upside cone whirling mode.

Some discrepancies between numerical and experimental results are noted in Fig. 11. The orbits in the bottom and upper planes obtained with the model are very similar to each other, showing a whirling mode of more cylindrical nature than that observed in experimentation. This can be explained by looking at the unbalance response function of the system (Fig. 12), obtained numerically. One can see in Fig. 12a that the cylindrical whirling mode (equal responses in the upper and bottom planes) occurs for frequency ratios ($\dot{\phi}/\omega_a$) around 0.81, which is the case of an absorber with 95 mm rods ($\omega_\alpha = 15.1$ Hz $\Rightarrow \dot{\phi}/\omega_a = 0.86$). Considering that, in the experimental results, the orbit in the upper plane is clearly smaller than that of the bottom plane, one can infer that the actual natural frequency of the absorber lies between 15.1 and 13 Hz (frequency ratios between 0.86 and 1.0 in Fig. 12).

In fact, the rods are not perfectly clamped on the top of the basket. The top of the basket is made of plastic material, and it has its own equivalent stiffness which is not high enough to allow a perfect clamping of the rods. As a consequence, it is reasonable to believe that the natural frequency of the absorber in the experiments is smaller than that predicted by theory. Consequently, this would result in a higher frequency ratio for the system.

In theory, according to Fig. 12a, a perfectly tuned absorber ($\dot{\phi}/\omega_a = 1.0$) in the washing machine would result in very small orbit amplitudes in the upper plane of the basket (anti-resonance location), but not as small orbit amplitudes in the bottom plane. The anti-resonance in the bottom of the basket only occurs at $\dot{\phi}/\omega_a = 1.12$, when the orbit amplitude in the upper plane has already increased. In order to have minimum orbit amplitudes in both planes of the basket (bottom and upper), a trade-off solution can be found between 1.0 and 1.12 frequency ratios ($11.6 < \omega_\alpha < 13$ Hz). But, in this frequency range, the bottom and the top of the basket would whirl in opposition of phase, as evidenced by phase information (Fig. 12b), representing another different whirling mode (bi-conical mode).

The first resonance of the system, due to the washing machine suspension, remains at 1.4 Hz ($\dot{\phi}/\omega_a = 0.1$). A second resonance appears in the system at 16.1 Hz ($\dot{\phi}/\omega_a = 1.24$), due to the presence of the absorber. Near the basket anti-resonances, the unbalance response of the absorber increases with increasing frequency ratio (74.2, 115.2, and 210.7 mm/kg m for $\dot{\phi}/\omega_a = 0.86$, 1.0, and 1.12, respectively). That means, the higher the frequency ratio is, the higher the orbit amplitude and stress on the rods are. Depending on the natural frequency of the absorber, one has to assure that loading stress in the absorber rods does not reach material yield limit of strength, as occurred in the case of study for the frequency ratio of 1.0. This could be achieved by changing the geometry of the elastic elements or by introducing more damping into the absorber system.

9 Conclusion

The application of a rotating ring dynamic absorber to a vertical axis washing machine is focused in this work. Although the studied absorber was not perfectly tuned to the rotating frequency of the machine, significant vibration reduction of the machine basket was numerically and experimentally observed. Based on the unbalance response of the system, obtained numerically, one can infer that further reduction of vibration amplitude is possible with better tuned absorbers. In this case, better tuned absorbers would have more impact in the upper plane of the basket, where the absorber is mounted, although vibration reduction in the bottom plane is also expected.

Care must be taken regarding system damping. In the case of this study, low damping in the absorber system prevented the investigation of a better tuned absorber. The vibration amplitude of the tuned absorber was high enough to cause stress in the rods (elastic elements), reaching their material yield limit of strength. As a consequence, the absorber system collapsed, and a slightly mistuned absorber had to be used. Considering the application in commercial washing machines, it is clear that the design of the absorber must be improved regarding geometry of the elastic elements and damping of the system. The concept, however, has been proven by the obtained results.

The mathematical model of the system presented good agreement with experimental results, especially in the case of the system with mistuned absorber. In the case of the absorber with 95 mm rods, the model predicted a larger effect of the absorber, concerning vibration reduction, than it really occurred experimentally. Part of this discrepancy can be credited to the assumption of perfect clamping of the rods on the top of the basket, which seems to be weak in face of the obtained results.

References

1. Alsuwaiyan AS, Shaw SW (2002) Performance and dynamics stability of general-path centrifugal pendulum vibration absorbers. J Sound Vib 252:791–815
2. Althaus J, Stelter P, Feldkamp B, Adam H (1993) Aktives hydraulisches Lager für eine Schneckenzentrifuge. Schwingungen in rotierenden Maschinen II—SIRM II, Wiesbaden, pp 28–36
3. Bae S, Lee JM, Kang YJ, Kang JS, Yun JR (2002) Dynamic analysis of an automatic washing machine with hydraulic balancer. J Sound Vib 257:3–18
4. Barrett LE, Gunther EJ, Allaire PE (1978) Optimum bearing and support damping for unbalance response and stability of rotating machinery. J Eng Power 100:89–94
5. Bavastri CA, Ferreira EMS, Espindola JJ, Lopes EMO (2008) Modeling of dynamic rotors with flexible bearings due to the use of viscoelastic materials. J Braz Soc Mech Sci Eng 30:22–29
6. Cheng CC, Wu FT, Hsu KS, Ho KL (2008) Design and analysis of auto-balancer of an optical disk drive using speed-dependent vibration absorbers. J Sound Vib 311:200–211
7. Horvath R, Flowers GT, Fausz J (2008) Passive balancing of rotor systems using pendulum balancers. J Vib Acoust 130:410111–4101111
8. Hibbeler RC (1994) Mechanics of materials. Prentice-Hall, Upper Saddle River, p 830
9. Ioriatti AS 2007 Dynamic study of vertical axis washing machines using multibody systems, Universidade de São Paulo, Escola de Engenharia de São Carlos, dissertation, p 114 (in Portuguese)
10. Johnson CD (1995) Design of passive damping systems. J Mech Des Spec 50th Anniv Des Issue 117:171–176
11. Johnson ME, Nascimento LP, Kasarda M, Fuller CR (2003) The effect of actuator and sensor placement on the active control of rotor unbalance. J Vib Acoust 125:365–373
12. Jorkama M, von Hertzen R (1998) Optimal dynamic absorber for a rotating rayleigh beam. J Sound Vib 217:653–664
13. Lee CT, Shaw SW, Copola VT (1997) Subharmonic vibration absorber for rotating machinery. J Vib Acoust 119:590–595
14. Miu DK (1991) Physical interpretation of transfer functions zeros for simple control systems with mechanical flexibilities. J Dyn Syst Meas Control 113:419–424
15. Nicoletti R, Santos IF (2005) Frequency response analysis of an actively lubricated rotor/tilting-pad bearing system. J Eng Gas Turbines Power 127:638–645
16. Olson BJ, Shaw SW, Pierre C 2005 Order-tuned vibration absorbers for cyclic rotating flexible structures. In: Proceedings of the ASME international design engineering technical conferences and computers and information in engineering conference—DETC2005, Long Beach, USA, pp 2475–2484
17. Rade DA, Silva LA (1999) On the usefulness of antiresonances in structural dynamics. J Braz Soc Mech Sci Eng 31:82–90
18. San Andres L, Lubell D (1998) Imbalance response analysis of a test rotor supported on squeeze-film dampers. J Eng Gas Turbines Power 120:397–404
19. Santos IF, Saracho CM, Smith JT, Elland J (2004) Experimental validation of linear and non-linear dynamic models for representing rotor-blade parametric coupled vibrations. J Sound Vib 271:883–904
20. Santos IF, Watanabe FY (2004) Compensation of cross-coupling stiffness and increase of direct damping in multirecess journal bearings using active hybrid lubrication—part i: theory. J Tribol 126:146–155
21. Sato Y (1990) Dynamic absorber using a hollow rotor partially filled with liquid. JSME Int J Ser 3: Vib Control Eng Eng Ind 33:446–452
22. Shaw SW, Schmitz PM, Haddow AG (2006) Tautochronic vibration absorbers for rotating systems. J Comput Nonlinear Dyn 1:283–293
23. Sun L, Krodkiewicks JM, Cen Y (1998) Self-tuning adaptive control of forced vibration in rotor systems using an active journal bearing. J Sound Vib 213:1–14
24. Vance JM, Li J (1996) Test results of a new damper seal for vibration reduction in turbomachinery. J Eng Gas Turbines Power 118:843–846